MJFAS MALAYSIAN JOURNAL OF FUNDAMENTAL AND APPLIED SCIENCES
PRINT ISSN: 2289-5981 | ONLINE ISSN: 2289-599X

RESEARCH ARTICLE

Phenol degradation behavior via photocatalytic of $ZnO/Ag_2CO_3/Ag_2O$ nanoparticles

Nurafiqah Rosman [a, b], Wan Norharyati Wan Salleh [a, b,*], Mohamad Azuwa Mohamed [c], Nor Hafiza Ismail [a, b], Nor Asikin Awang [a, b], Ahmad Fauzi Ismail [a, b], Juhana Jaafar [a, b], Zawati Harun [d]

[a] *Advanced Membrane Technology Research Centre (AMTEC), Universiti Teknologi Malaysia, 81310 Skudai, Johor, Malaysia*
[b] *Faculty of Chemical and Energy Engineering, Universiti Teknologi Malaysia, 81310 Skudai, Johor, Malaysia*
[c] *Centre of Advanced Materials and Renewable Resources (CAMARR), Faculty of Science and Technology, Universiti Kebangsaan Malaysia, 43600 UKM Bangi, Selangor, MALAYSIA*
[d] *Integrated Material and Process, Advanced Materials and Manufacturing Centre (AMMC), Faculty of Mechanical and Manufacturing Engineering, Universiti Tun Hussein Onn Malaysia, 86400 Parit Raja, Batu Pahat, Johor Darul Takzim, Malaysia*

* *Corresponding author: hayati@petroleum.utm.my*

Article history
Received 7 Mac 2019
Revised 20 May 2019
Accepted 10 September 2019
Published Online

Graphical abstract

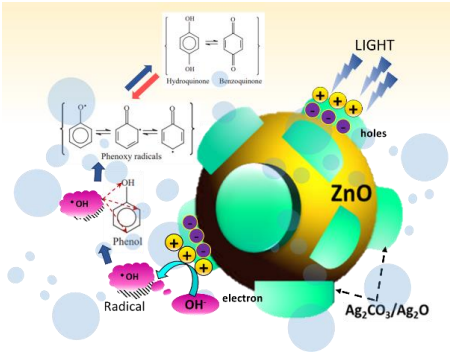

Abstract

The present study successfully conducted the synthesis of $ZnO/Ag_2CO_3/Ag_2O$ nanocomposite using co-precipitate technique and phase transformation route. The resulting nanocomposite photocatalyst were characterized by TEM and UV–vis spectra, while their photocatalytic activities were subsequently tested in the mineralization of phenol solution. Meanwhile, the heterojunction of Ag_2CO_3/Ag_2O over ZnO lattice that influenced the surface-phase structure of the nanocomposites managed to generate higher absorption in visible light region in UV NIR spectra. In addition, the surface phase structure was produced via Ag_2O crystal growth over Ag_2CO_3 which was heterojunctioned on ZnO lattice, thus leading to an effective charge carrier transfer that indirectly suppressed the recombination of photogenerated electrons and holes. The results of the current research on the photocatalytic behaviour of the nanocomposites demonstrated that the phenol peak area for $ZnO/Ag_2CO_3/Ag_2O$ under UV light decreased 25.4 % compared to visible light radiation of 14.1 %. The presence of photo-oxidation products was detected in the liquid phase products in phenol-oxidation even though phenol was not completely removed. Overall, it was remarkable to discover that the formation of Ag_2CO_3/Ag_2O mixed phase heterojunction over the surface of ZnO significantly enhanced the photocatalytic activity under visible light irradiation.

Keywords: Photocatalysis, phenol degradation, heterostructure, ZnO, Ag_2CO_3/Ag_2O

INTRODUCTION

Semiconductor photocatalysts have attracted considerable attention for the past decades in regard to the conversion of light energy to chemical energy, particularly involving environmental purification and solar energy conversion. Generally, ZnO appears to be one of the most promising and suitable materials for photocatalysis due to its high photoactive features, biologically and chemically inert, and reasonably low cost (Guo *et al.*, 2011). However, ZnO can only be excited at ultraviolet or near-ultraviolet irradiations which prevents it from being applied in visible light photocatalyst application (Miguel Pelaez *et al.*, 2012). In regard to this matter, recent evidence suggests that Ag-based semiconductor photocatalysts such as AgBr (Zhang *et al.*, 2014), Ag_3PO_4 (Li *et al.*, 2014), AgI (Zeng, 2013), and Ag_2CO_3 (Donga, 2013) are able to significantly enhance photocatalytic performance due to their photosensitivity towards visible light.

Nevertheless, it should be noted that silver-containing materials tend to exhibit small band gap which subsequently leads to electron-hole pairs recombination as well as lower photocatalytic activity performance (Habibi-Yangjehn & Pirhashemi, 2015; Wang *et al.*, 2013). However, it is believed that the condition can be overwhelmed via silver semiconductors heterojunction using a low-cost semiconductor such as ZnO. Previous studies have proven that photocatalysts with well-defined junctions between the two semiconductors along with matched electronic band structures can result in enhanced photocatalytic performance. More importantly, the structures can effectively facilitate charge transfer and suppress the recombination of photogenerated electrons and holes with the aim of achieving high activity and stability (Habibi-Yangjeh & Pirhashemi, 2016; Wang *et al.*, 2014; Yan *et al.*, 2014). On another note, several past studies have investigated the photocatalytic activities under visible-light irradiation for binary ZnO-containing different photocatalysts such as ZnO/AgBr, ZnO/Ag_2CO_3, ZnO/Ag_3PO_4, ZnO/AgI, and ZnO/Ag_2CrO_4 (Krishnakumar *et al.*, 2012; Dong *et al.*, 2014; Habibi-Yangjeh & Mahsa Pirhashemi, 2016; Shaker-Agjekandy *et al.*, 2015; Wun *et al.*, 2014).

Recently, the activity of binary photocatalyst was able to be significantly upgraded by adding an appropriate narrow band gap semiconductors for the purpose of fabricating the ternary photocatalyst (Golzad-Nonakaran *et al.*, 2016; Habibi-Yangjehn &

Mahsa Pirhashemi, 2015; Rong *et al.*, 2016). Moreover, the findings of the studies revealed that the heterojunction of Ag_2CO_3 over ZnO is able to form an n-n heterostructure that leads to a remarkable charge separation efficacy with the aim of enhancing life-time charge pairs (Habibi-Yangjeh *et al.*, 2016; Pirhashemi & Habibi-Yangjeh, 2016). Interestingly, Ag_2CO_3 tends to form mixed phase structure which involves a transition stage of the phase transformation from Ag_2CO_3 to Ag_2O. Furthermore, Yu *et al.* (2014) have discovered well-defined junctions between Ag_2CO_3 and Ag_2O with an n-type narrow band gap semiconductors through facile phase transformation that is capable of producing extremely high activity and stability. This finding demonstrates a direct correlation between the surface phases of Ag_2CO_3 during the heterojunctioning of ZnO particles.

In the current work, the $ZnO/Ag_2CO_3/Ag_2O$ nanocomposite was prepared using two stage methods which were co-precipitate and facile phase transformation method based on the thermal decomposition of Ag_2CO_3. Next, the nanocomposite was characterized using the transmission electron microscopy (TEM) and UV NIR Spectrometer with the aim of understanding the relation between the structure and properties of the ternary photocatalyst product. Finally, the photocatalytic decomposition behavior of phenol over $ZnO/Ag_2CO_3/Ag_2O$ nanocomposite was investigated under UV and visible irradiation using high performance liquid chromatography (HPLC).

EXPERIMENTAL

Materials

The starting materials which include zinc acetate dihydrate ($C_4H_6O_4Zn{\cdot}_2H_2O$, HmbG), silver nitrate ($AgNO_3$, Sigma Aldrich), and sodium bicarbonate ($NaHCO_3$, Bendosen) were respectively utilized as the precursor for ZnO, Ag_2CO_3, and Ag_2O. The phenol used in the present study was obtained from Sigma Aldrich without further purification, while all solutions were prepared using RO water.

Synthesis of $ZnO/Ag_2CO_3/Ag_2O$ nanocomposite

First, pure ZnO was prepared by grinding 10.0 g of $Zn(Ac)_2{\cdot}2H_2O$ (HmbG) for 30 minutes and calcined at 450 °C at the heating rate of $10°C.min^{-1}$ for 2 hours under air atmosphere. The heterojunction of Ag_2CO_3 over ZnO crystal lattice was performed by utilizing 1.5 g pure ZnO which was then dissolved into 40 mL $NaHCO_3$ (0.336 g, Bendosen) solution under stirring. Next, 20 mL of $AgNO_3$ (1.358 g, Sigma Aldrich) solution was slowly added dropwise into the solution and left stirred for 24 hours under room temperature. Meanwhile, the grayish yellow suspension was then filtered and washed three times with deionized (DI) water and dried at 60 °C overnight. Finally, the ZnO/Ag_2CO_3 was calcined at 195 °C for 8 minutes under atmospheric pressure and taken out immediately. The synthesis process is illustrated in Fig. 1.

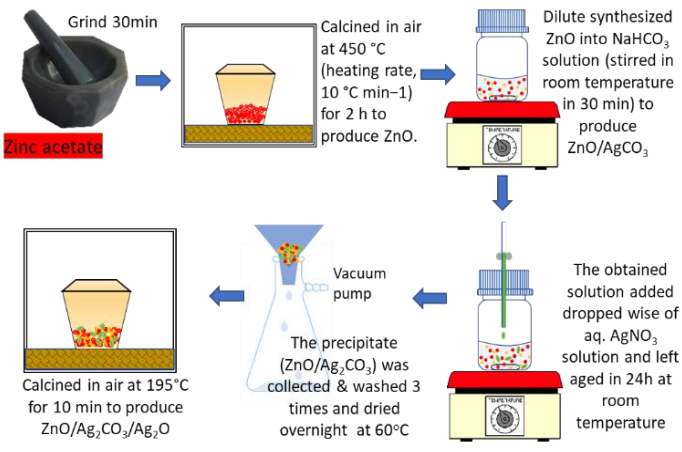

Fig. 1 Schematic diagram for preparation of $ZnO/Ag_2CO_3/Ag_2O$.

Characterization

The phase evaluation of $ZnO/Ag_2CO_3/Ag_2O$ nanocomposite was performed using transmission electron microscopy (TEM JEM-ARM 200F) and X-ray Diffraction (Siemens X-ray diffractometer D5000) at 40 kV and 40 mA for monochromatized Cu K α (λ = 0.15406 Å) radiation. In the present study, the optical property of $ZnO/Ag_2CO_3/Ag_2O$ nanocomposite was analyzed using a UV-vis-NIR spectrophotometer (UV-3600 Plus Shidmadzu). For photocatalytic evaluation, the phenol photodegradation efficiency of $ZnO/Ag_2CO_3/Ag_2O$ nanocomposite was tested under UV and visible light irradiation. Meanwhile, reaction suspensions were prepared by adding 0.1 g of catalysts to 200 mL of aqueous phenol solution with an initial concentration of 50 ppm, in which the solution mixture was stirred for 1 h in the dark to achieve equilibrium adsorption. The test was carried out using ultraviolet (UV) lamp (Vilber Laurmat, l = 312 nm, 30 W) and visible light with white light-emitting diode (LED) spot light (> 420 nm, 100 W). Next, the samples were collected at regular intervals from the suspension, while the photocatalyst was removed using the spectrophotometer at 270 nm which corresponded to the maximum absorption wavelengths of phenol prior to the analysis. In the present study, the photodegradation efficiency was calculated using Eq. (1) presented as follows:

$$Photodegradation\ efficiency\ (\%) = (1- C_t/C_0) \times 100 \quad (1)$$

where C_0 describes the concentration of phenol before illumination, while C_t denotes the concentration of phenol solution at time illumination (t). On another note, the pseudo-first order expressed in Eqn. 2 has been generally adopted for photocatalytic degradation to quantitatively determine the phenol degradation. The first order rate constant (k) of the photocatalytic reaction is presented below:

$$ln(C_t/C_o) = k\,t \quad (2)$$

where C_0 and C_t refer to the concentrations of phenol at the respective irradiation time 0 and t min, while k represents the apparent pseudo-first-order rate constant.

RESULTS AND DISCUSSION

Physicochemical properties of $ZnO/Ag_2CO_3/Ag_2O$

As presented in Fig. 2, the phase structure of $ZnO/Ag_2CO_3/Ag_2O$ for the present study was evaluated using TEM (JEM-ARM 200F). The actions shown occurred at the grain boundary involving the mixed grains of Ag_2CO_3 and Ag_2O during the calcination process performed at 195 °C in 8 minutes. However, no clear lattice fringe of Ag_2CO_3 can be observed in TEM images of $ZnO/Ag_2CO_3/Ag_2O$ which is believed to be the result of the thermally unstable Ag_2CO_3 that leads to the partial decomposition of Ag_2CO_3 to Ag_2O during calcination reaction (Koga *et al.*, 2013; Yu *et al.*, 2014). In the present study, only ZnO and Ag_2O clear lattice fringe nanocrystals could be detected. On a more important note, the measurement of lattice nanocrystals has led to the measurement of the resolved interplanar distance of ZnO and Ag_2O which are respectively recorded as 0.27 nm and 0.25 nm. In addition, both are revealed to resemble (101) and (111) planes of Ag_2O.

Fig. 3 illustrates the crystallinity and validation of $ZnO/Ag_2CO_3/Ag_2O$ samples that were carried out using X-ray diffraction (XRD). In this case, it can be observed that the diffraction peaks of ZnO in $ZnO/Ag_2CO_3/Ag_2O$ nanocomposite can be indexed to the pure hexagonal phase of wurtzite-type ZnO (JCPDS no. 05 0664). Meanwhile, the XRD pattern of $ZnO/Ag_2CO_3/Ag_2O$ demonstrates the characteristic peaks that respectively adhere to cubical Ag_2O (111) and (011) planes at 32.79° and 38.07°, which show the conversion of Ag_2CO_3 to Ag_2O. In fact, Ag_2CO_3 that was calcined at 195 °C for 8 min displays the diffraction peaks for both cubic phases of Ag_2O as well as the monoclinic structure of Ag_2CO_3, which consequently leads to the formation of Ag_2CO_3/Ag_2O composite phases on ZnO. In addition, Ag_2CO_3 that was transformed into Ag_2O can be elucidated by increasing the heat duration for Ag_2CO_3 oxidation processes (Yu *et al.*, 2014). However, Ag_2CO_3 is present and can be readily indexed to

monoclinic phase Ag_2CO_3, while the diffraction peaks are indexed to specific (hkl) based on the JCPDS no. 26 0339.

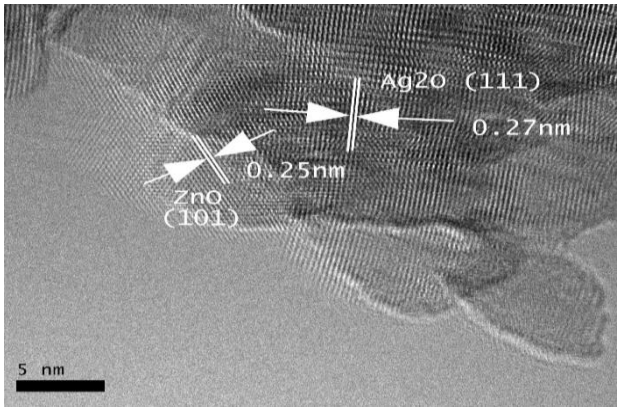

Fig. 2 High resolution of TEM image of ZnO heterojunction with Ag_2CO_3/Ag_2O mixed phase nanocomposite.

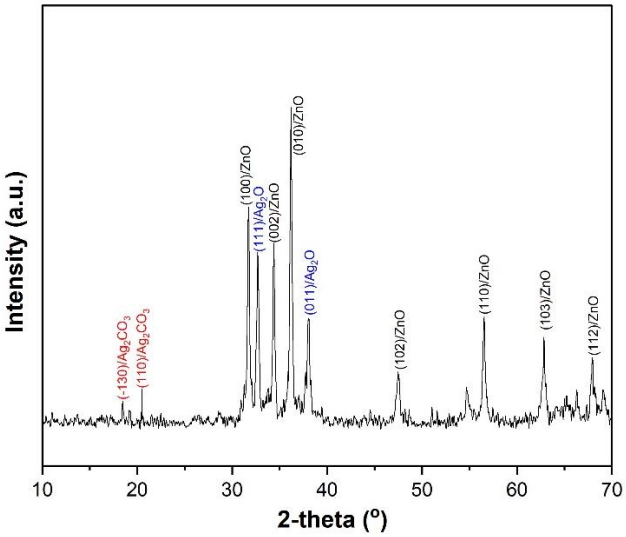

Fig. 3 XRD patterns of the, $ZnO/Ag_2CO_3/Ag_2O$ nanocomposite.

Furthermore, the optical properties of $ZnO/Ag_2CO_3/Ag_2O$ nanocomposite in the present study were examined using UV-Vis absorption spectrometer (UV-3600 Plus Shidmadzu) and the results are shown Fig. 4. The heterostructured photocatalysts manage to demonstrate an excellent optical response to UV and visible region compared to pure ZnO photocatalyst. A possible explanation to this may be due to the smaller band gap possessed by Ag_2CO_3 and Ag_2O that is able to effortlessly excite electrons, thus enabling greater absorption in the visible light region (Golzad-Nonakaran *et al.*, 2016; Wu *et al.*, 2014). As can be observed in the same figure, the estimated band gap values of ZnO and $ZnO/Ag_2CO_3/Ag_2O$ are respectively shown to be approximately 3.05 and 2.77 eV. More importantly, it would also be useful in separating the photogenerated electron-hole pairs through the heterojunction of both Ag_2CO_3 and Ag_2O over ZnO crystal lattice.

Other than that, the findings showed that ZnO has the highest negative potential at conduction band, followed by Ag_2O and then Ag_2CO_3. Hence, this indicates that the photogenerated electrons in ZnO and Ag_2O can be easily transferred to the surface of the Ag_2CO_3 and holes are seen to be present on the surface. Meanwhile, it is important to note that the photoinduced holes on the surface of ZnO and Ag_2CO_3 visualized in Fig. 5 can migrate to the Ag_2O surface in order to promote effective separation of photoexcited electrons and holes, thus reducing the probability of electron–hole recombination (Lee *et al.*, 2016; Chong *et al.*, 2010). Therefore, it can be observed that the charge carriers are effectively separated due to the formation of Ag_2CO_3/Ag_2O heterojunctions between ZnO with two narrow band gap semiconductors. As a result, this increases the life time of the electron–hole pairs which leads to more production of •OH and $•O^2$ for the purpose of decomposing the organic pollutants efficiently. However, as shown in Fig. 4, the electron-hole pairs of ZnO are unable to be excited under visible light due to weak photogenerated electron-hole pairs that can only be generated under UV illumination.

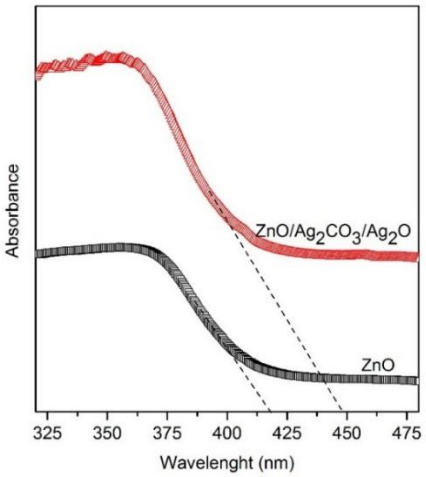

Fig. 4 UV–visible absorption spectrum of ZnO and $ZnO/Ag_2CO_3/Ag_2O$ nanocomposites.

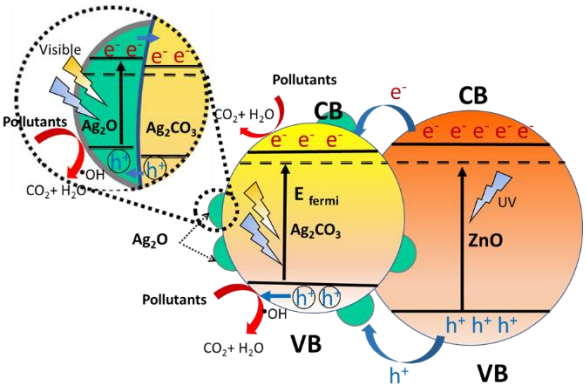

Fig. 5 Schematic photocatalytic reaction processes and charge transfer of $ZnO/Ag_2CO_3/Ag_2O$ nanocomposites under light illumination.

Evaluation of photocatalytic activity

A photocatalyst that that can be activated by visible or UV light for the purpose of producing an efficient photocatalytic degradation of pollutant waste is deemed important in generating hydroxyl radical (•OH). The UV vis spectra of $ZnO/Ag_2CO_3/Ag_2O$ showed that the extension of absorption band was shifted to the visible region. Therefore, phenol degradation under UV and visible light was evaluated in order to examine the effectiveness of $ZnO/Ag_2CO_3/Ag_2O$ nanocomposite.

Fig. 6 (a) shows the photodegradation efficiency of ZnO and $ZnO/Ag_2CO_3/Ag_2O$ under UV light. The results show that the oxidization of phenol for photodegradation efficiency of $ZnO/Ag_2CO_3/Ag_2O$ is higher under UV or visible light irradiation compared to ZnO photocatalyst. In particular, it can be observed that the phenol degradation using $ZnO/Ag_2CO_3/Ag_2O$ of 56.00 % and 41.40 % are recorded for UV and visible light irradiation, respectively. On the other hand, the results of phenol degradation for ZnO are 41.45 % and 20.37 % under UV and visible light, respectively. Meanwhile, Fig. 6 (b) shows the linear plots of $-\ln(C_t/C_o)$ of ZnO and $ZnO/Ag_2CO_3/Ag_2O$ nanocomposites with respect to the irradiation time under UV and visible radiation. According to the slope of the $ZnO/Ag_2CO_3/Ag_2O$ linear fitted graph, the calculated k values are shown to be higher than ZnO with 18.5 and 13.4 E-4 min^{-1} for UV and visible light, respectively. Meanwhile, ZnO only achieves 12.8 and 4.8 E-4 min^{-1} for UV and visible light, respectively. Hence, these results suggest that the $ZnO/Ag_2CO_3/Ag_2O$

nanocomposite has higher reaction rate of phenol degradation under UV and visible light as tabulated in Table 1. The lower degradation of ZnO under visible or UV light irradiation was resulted by the limitation of ZnO in generating electron-holes under both light irradiations.

Nevertheless, it is important to note that $ZnO/Ag_2CO_3/Ag_2O$ nanocomposite prefers to perform under UV light irradiation considering that photogenerated electrons of ZnO and Ag_2O can easily be transferred to Ag_2CO_3 surface, which subsequently leaves holes on the surface to enable •OH and $•O^2$ to be produced. However, the electron-holes generation can only be produced by Ag_2O under visible illumination, thus causing the reaction rate of phenol oxidation to be less effective compared to UV radiation.

Table 1 Kinetic fit and percentage of phenol degradation using ZnO and $ZnO/Ag_2CO_3/Ag_2O$ nanocomposite under UV and visible light irradiation.

Photocatalyst	Light Source	K (E-4 min^{-1})	Photodegradation (%)
ZnO	UV	12.8	41.45
$ZnO/Ag_2CO_3/Ag_2O$		18.5	56.00
ZnO	Visible	4.8	20.37
$ZnO/Ag_2CO_3/Ag_2O$		13.4	41.40

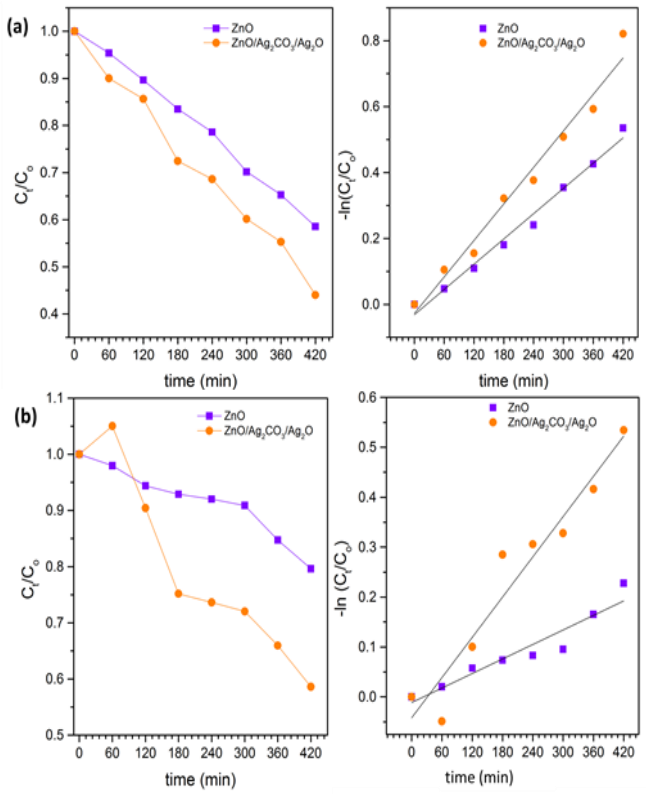

Fig. 6 Photodegradation and kinetic fit of phenol over ZnO and $ZnO/Ag_2CO_3/Ag_2O$ nanocomposites under (a) UV; and (b) visible light

Next, HPLC test was conducted to identify the trend of phenol degradation and the presence of intermediate compound produced from the process of phenol photo-oxidation. In Fig. 7 (a), the maximum peak height at 254 nm absorption chromatogram shows that the phenol is eluted at 3.1 minutes. It is crucial to note that the area of the phenol peak decreases by 25.4 % and slightly shifted to the left over a 7-hours of reaction time, which is accompanied by the presence of benzoquinone and hydroquinone at 1.7 and 2.0 min, respectively as suggested by Mu`azu and Al-Malack (2012).

In addition, the peak that corresponds to phenol is still exhibited after 7-hour of UV irradiation, thus indicating that it is not completely degraded.

In addition, the visible light irradiation of the $ZnO/Ag_2CO_3/Ag_2O$ nanocomposite over phenol solution shown in Fig. 7 (b) reveals that the $ZnO/Ag_2CO_3/Ag_2O$ exhibits a dissimilar pattern peak area for phenol photo-oxidation. Moreover, the peak area is shown to decrease by 14.1 % with an identical peak shape, while phenol photo-oxidation or intermediate products tend to perform differently for $ZnO/Ag_2CO_3/Ag_2O$ that is irradiated under visible light. Hence, this suggests that the $ZnO/Ag_2CO_3/Ag_2O$ is not able to generate a significant amount of •OH under UV irradiation. Apart from that, this also indicates that ZnO is unable to excite valance electron under visible light which leads to lower photocatalytic degradation considering that it can only be activated under UV light irradiation. Therefore, the phenol oxidation process under visible light tends to occur less in visible light irradiation.

According to Fig. 7(b), a slight presence of catechol at 2.2 min can be observed in visible light irradiation following the comparison performed on both intermediate compounds produced after 7hr of light irradiation. Hence, it can be indicated that the catechol is not fit to perform the next phase of phenol degradation transition (refer to Scheme 1). However, the transformation of catechol or hydroquinone is able to generate benzoquinone formation. In this case, it can be seen that benzoquinone peak is higher in UV light radiation compared to visible light due to the presence of larger oxidant radical.

Furthermore, the phenol solutions also exhibited color changes during the photo-oxidation process that can be observed by naked eyes. The liquid turned into brown yellow in the first 30 minutes of phenol oxidation. Next, the brown yellow color faded to yellow color during the continuous visible light radiation, but the color almost disappeared after 4 hours. In this case, the yellow color is characteristically believed to be caused by benzoquinone that is produced by phenol oxidation (Comninellis & Pulgarin, 1991).

However, it is crucial to note that the color transition of phenol liquid under UV radiation occurred almost throughout the entire process of the experiment. The phenol liquid started with concentrated yellowish brown color which then turned into brown yellow, but faded to yellow at the end of the process. This can be clearly observed in Fig. 7(b) whereby the benzoquinone peak is shown to have higher HPLC.

On another note, it is believed that more generation of •OH on the excited ZnO nanocomposite surface under UV radiation tends to produce higher phenol photo-oxidation compared to visible light radiation. A possible explanation to this may refer to the ability of ZnO to generate •OH under UV light irradiation, which subsequently increases the oxidation process. Therefore, phenol oxidation and the generation of intermediate compound remain to occur. Apart from that, the color transition validated that phenol molecules were initially oxidized through the reaction of •OH on the excited ZnO nanocomposite surface, which further promotes the reaction.

Meanwhile, it is crucial to note that phenol degradation was not completely degraded to biodegradable substance even though the color of the phenol changed into colourless based on the result of HPLC chromatogram. A possible explanation to this may be due to the fact that phenol can only be transformed into hydroquinone that is colourless. As suggested by Rieger (1987), benzoquinone and hydroquinone are known as an active redox couple in equilibrium in an aqueous solution. According to the HPLC results, it can be indicated that the transformation of the phenol is caused by $ZnO/Ag_2CO_3/Ag_2O$ nanocomposite performed under visible and UV light radiation. Overall, both photo-oxidation processes manage to degrade phenol into benzoquinone and hydroquinone based on photo-oxidation products or intermediate compounds as illustrated in Fig. 7.

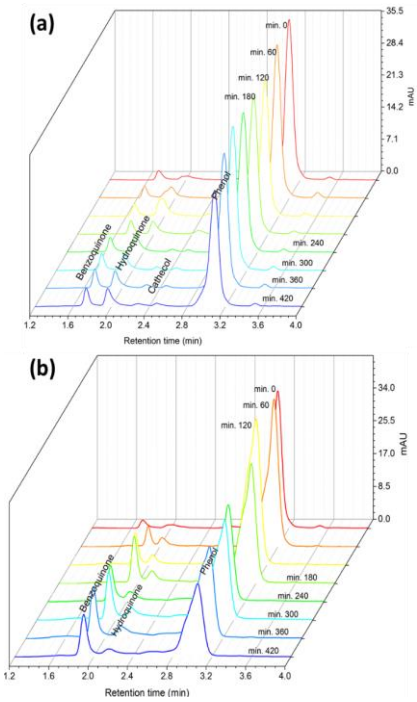

Fig. 7 HPLC–MS representative analysis of $ZnO/Ag_2CO_3/Ag_2O$ under (a) UV and (b) visible light irradiation at different running times.

According to HPLC analysis, Scheme 1 shows that the color changes which occurred during phenol illumination may be caused by phenol degradation for the proposed phenol-oxidation pathway. Basically, phenol molecule initially underwent the oxidation reaction through •OH on the excited ZnO nanocomposite surface. These •OH attacked the phenyl ring that yielded hydroquinone, resorcinol, and catechol which are colored intermediate compounds (Seftel, 2014; Pardeshi and Patil, 2008). Therefore, this caused hydroquinone to be degraded to colorless benzoquinone based on the color transition occurred in the experiment.

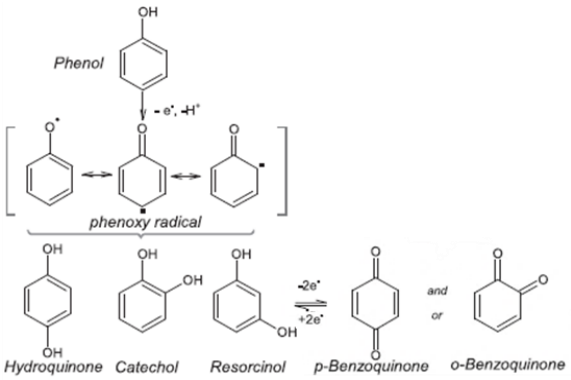

Scheme 1 Proposed photo-degradation pathway of phenol.

CONCLUSION

The results of the present study showed that the photocatalytic activity of $ZnO/Ag_2CO_3/Ag_2O$ nanocomposite was related to the surface-phase structure and optical properties which were respectively characterized by high resolution TEM and UV Vis spectra. The heterojunction of Ag_2O/Ag_2CO_3 over ZnO particles demonstrated the harvesting of more visible light due to the increase of the function of mixed phase photocatalyst efficiency based on the optical capability of $ZnO/Ag_2CO_3/Ag_2O$ in the entire range of visible region in UV Vis spectra. Other than that, the photocatalytic activity of phenol indicated that the performance of $ZnO/Ag_2CO_3/Ag_2O$ was more successful under UV irradiation compared to visible radiation. However, this resulted in the formation of Ag_2CO_3/Ag_2O mixed phase heterojunctioned over ZnO nanocomposites that managed to be performed with 41.3 % phenol degradation in visible light radiation. However, it can be concluded that Ag_2CO_3/Ag_2O heterojunction into ZnO nanoparticles still managed to produce a significant degradation even though the phenol compound failed to be completely degraded based on the transitions of colored intermediate compounds during visible illumination.

ACKNOWLEDGEMENT

This work was financially supported by the Universiti Teknologi Malaysia under the Research University Grant (Project Number: Q.J130000.2546.3551.05G76) and Ministry of Education Malaysia under HICoE Scheme Grant (Project Number: RJ090301. 7846.4J187).

REFERENCES

Chong M. N., Christopher, B. J., Chow, W. K., Saint, C. (2010). Recent developments in photocatalytic water treatment technology: A review. *Water Research, 44*(10), 2997-3027.

Comninellis, Ch., Pulgarin, C. (1991). Anodic oxidation of phenol for waste water treatment. *Journal of Applied Electrochemistry*, *21*(8), 703-708.

Dong, C., Wu, K. L., Li, M. R., Li, L., Wei, X. (2014). Synthesis of Ag_3PO_4–ZnO nanorod composites with high visible-light photocatalytic activity. *Catalysis Communications, 46*, 32–35.

Donga, G. C., Sun, J., Li, C., Yu, Y., Chen, D. (2013). A novel high-efficiency visible-light sensitive Ag_2CO_3 photocatalyst with universal photodegradation performances: Simple synthesis, reaction mechanism and first-principles study. *Applied Catalysis B: Environmental, 134–135*, 46-54.

Golzad-Nonakaran B., Habibi-Yangjeh, A. (2016). Ternary $ZnO/AgI/Ag_2CO_3$ nanocomposites: Novel visible-light-driven photocatalysts with excellent activity in degradation of different water pollutants. *Materials Chemistry and Physics, 184*, 210-221.

Guo, T., Liu, Y., Zhang, Y., Zhang, M. (2011). Green hydrothermal synthesis and optical absorption properties of ZnO_2 nanocrystals and ZnO nanorods. *Material Letters, 65*(4), 639–641.

Habibi-Yangjeh, A., Shekofteh-Gohari, M. (2016). $Fe_3O_4/ZnO/Ag_3VO_4/AgI$ nanocomposites: Quaternary magnetic photocatalysts with excellent activity in degradation of water pollutants under visible light. *Separation and Purification Technology, 166*, 63-72.

Krishnakumar, B., Subash, B., Swaminathan, M. (2012). AgBr–ZnO – An efficient nano-photocatalyst for the mineralization of Acid Black 1 with UV light. *Separation and Purification Technology, 85*, 35–44.

Koga, N., Yamada, S., Kimura, T. (2013). Thermal decomposition of silver carbonate: Phenomenology and physicogeometrical kinetics. *The Journal of Physical Chemistry C, 117*(1), 326−336.

Lee, K. M., Lai, C. W., Ngai, K. S., Juan, J. C. (2016). Recent developments of zinc oxide based photocatalyst in water treatment technology: A review. *Water Research, 88*, 428-448.

Li, X.,Wu, K., Dong, C., Xia, S., Ye, Y., Wei, X. (2014). Size-controlled synthesis of Ag_3PO_4 nanorods and their high-performance photocatalysis for dye degradation under visible-light irradiation. *Materials Letters, 130*, 97-100.

Pelaez, M., Nolan, N., Pillai, S., Seery, M., Falaras, P., Kontos, A. G., Dunlop, Patrick S. M., Hamilton, J. W. J., Byrne, J. A., O'Shea, K., Entezari, M. H., Dionysioua, D. D.(2012). A review on the visible light active titanium dioxide photocatalysts for environmental applications. *Applied Catalysis B: Environmental, 125*, 331-349.

Morales-Flores, N., Pal, U., Sánchez Mora, E. (2011). Photocatalytic behavior of ZnO and Pt-incorporated ZnO nanoparticles in phenol degradation. *Applied Catalysis A: General, 394*(1-2), 269-275.

Mu`azu, N. D., Al-Malack, M. H. (2012). Influence of some operating parameter on electro-oxidation of phenol using boron doped diamond anode and graphite cathode. *Journal of Environmental Science and Technology*, *5*(6); 460-474.

Pardeshi, S. K., Patil, A. B. (2008). A simple route for photocatalytic degradation of phenol in aqueous zinc oxide suspension using solar energy. *Solar Energy*, *82*(8), 700-705.

Pirhashemi, M., Habibi-Yangjeh, A. (2015). Ternary $ZnO/AgBr/Ag_2CrO_4$ nanocomposites with tandem n–n heterojunctions as novel visible-light-driven photocatalysts with excellent activity. *Ceramics International, 41*(10), 14383–14393.

Pirhashemi, M., Habibi-Yangjeh, A. (2016). Novel ZnO/Ag_2CrO_4 nanocomposites with n–n heterojunctions as excellent photocatalysts for degradation of different pollutants under visible light. *Journal of Materials Science: Materials in Electronics, 27*(4), 4098–4108.

Pirhashemi, M., Habibi-Yangjeh, A. (2016). Photosensitization of ZnO by AgBr and Ag_2CO_3: Nanocomposites with tandem n-n heterojunctions and highly enhanced visible-light photocatalytic activity. *Journal of Colloid and Interphase Science, 474*, 103-113.

Rieger, M. (1987). The chemical fate of antioxidants. *Cosmet Toilet*, *102*, 83-96.

Rong, X., Qiu, F., Jiang, Z., Rong, J., Pan, J., Zhang, T., Yang, D. (2016). Preparation of ternary combined ZnO-Ag_2O/porous g-C_3N_4 composite photocatalyst and enhanced visible-light photocatalytic activity for degradation of ciprofloxaci. *Chemical Engineering Research and Design, 111*, 253–261.

Seftel, E. M., Mertens, M., Cool, P., Carja, G. (2014). Assemblies of nanoparticles of CeO_2–ZnTi-LDHs and their derivedmixed oxides as novel photocatalytic systems for phenol degradation. *Applied Catalysis B: Environmental, 150– 151,* 157– 166.

Shaker-Agjekandy, S., Habibi-Yangjeh, A. (2015). Facile one-pot method for preparation of AgI/ZnO nanocomposites as visible-light-driven photocatalysts with enhanced activities. *Materials Science in Semiconductor Processing, 34*, 74-81.

Wang, W., Wang, J., Wang, Z., Wei, X., Liu, L., Ren, Q., Shi, H. (2014). p-n junction CuO/BiVO4 heterogeneous nanostructures: Synthesis and highly efficient visible-light photocatalytic performance. *Dalton Transactions, 43*(18), 6735-6743.

Wu, C. (2014). Synthesis of Ag_2CO_3/ZnO nanocomposite with visible light-driven photocatalytic activity. *Materials Letters, 136*, 262-264.

Wang, Y., Wang, Q., Zhan, X., Wang, F., Safdar, M., He, J. (2013). Visible light driven type II heterostructures and their enhanced photocatalysis properties: A review. *Nanoscale, 5*(18), 8326-8339.

Yan Y, H. G., Song Liua, Rongying Jianga. (2014). Ag_3PO_4/Fe_2O_3 composite photocatalysts with an n–n heterojunction semiconductor structure under visible-light irradiation. *Ceramics International, 40*(7), part A, 9095–9100.

Yu, C., Li, G., Kumar, S., Yang, K., Jin, R. (2014). Phase transformation synthesis of novel Ag_2O/Ag_2CO_3 heterostructures with high visible light efficiency in photocatalytic degradation of pollutants. *Advanced Materials, 26*(6), 892-898.

Zeng, C., Zhang, B. T. J. (2013). Silver halide/silver iodide@silver composite with excellent visible light photocatalytic activity for methyl orange degradation. *Journal of Colloid and Interphase Science, 405*, 17-21.